Generation of hypoimmunogenic human pluripotent stem cells

Xiao Han[a,b], Mengning Wang[a,b,1], Songwei Duan[a,b,1], Paul J. Franco[a,b], Jennifer Hyoje-Ryu Kenty[a,b], Preston Hedrick[a,b], Yulei Xia[a,b], Alana Allen[a,b], Leonardo M. R. Ferreira[a,b,c], Jack L. Strominger[a,b,2], Douglas A. Melton[a,b], Torsten B. Meissner[a,b,d,e,2], and Chad A. Cowan[a,b,d,e,f,2]

[a]Department of Stem Cell and Regenerative Biology, Harvard University, Cambridge, MA 02138; [b]Harvard Stem Cell Institute, Harvard University, Cambridge, MA 02138; [c]Department of Molecular and Cellular Biology, Harvard University, Cambridge, MA 02138; [d]Division of Cardiovascular Medicine, Beth Israel Deaconess Medical Center, Boston, MA 02115; [e]Department of Medicine, Harvard Medical School, Boston, MA 02115; and [f]Broad Institute of MIT and Harvard, Cambridge, MA 02142

Contributed by Jack L. Strominger, March 27, 2019 (sent for review February 12, 2019; reviewed by Marco Colonna and David H. Sachs)

Polymorphic HLAs form the primary immune barrier to cell therapy. In addition, innate immune surveillance impacts cell engraftment, yet a strategy to control both, adaptive and innate immunity, is lacking. Here we employed multiplex genome editing to specifically ablate the expression of the highly polymorphic HLA-A/-B/-C and HLA class II in human pluripotent stem cells. Furthermore, to prevent innate immune rejection and further suppress adaptive immune responses, we expressed the immunomodulatory factors PD-L1, HLA-G, and the macrophage "don't-eat me" signal CD47 from the *AAVS1* safe harbor locus. Utilizing in vitro and in vivo immunoassays, we found that T cell responses were blunted. Moreover, NK cell killing and macrophage engulfment of our engineered cells were minimal. Our results describe an approach that effectively targets adaptive as well as innate immune responses and may therefore enable cell therapy on a broader scale.

HLA allobarrier | NK cells | macrophages | cell therapy | stem cell engineering

A major obstacle for cell therapy is the rejection of allogeneic cells by the recipient's immune system. However, multiple limitations prohibit the broader use of banking cells with defined HLA haplotypes and patient-specific induced pluripotent stem cells (iPSCs) (1, 2), emphasizing the need for "off-the-shelf" universal cell products. Ablating the highly polymorphic HLA class Ia and class II molecules is necessary to prevent the activation of cytotoxic $CD8^+$ T and $CD4^+$ T helper cells. Recently, the power of the CRISPR/Cas9 genome-editing system provided us and others with a tool to interfere with HLA class I expression in human pluripotent stem cells (hPSCs) or hematopoietic cells by knocking out the accessory chain beta-2-microglobulin (B2M) (3–7) and to eliminate HLA class II expression by targeting its transcriptional master regulator, CIITA (7, 8). However, the deletion of B2M also prevents the surface expression of the nonpolymorphic HLA class Ib molecules HLA-E and HLA-G, which are required to maintain NK cell tolerance (9, 10). Therefore, individual deletion of the HLA-A/-B/-C genes may represent a more favorable strategy to protect the donor cells from $CD8^+$ T cell-mediated cytotoxicity without losing the HLA class Ib protective function.

It has previously been shown that the T cell checkpoint inhibitors PD-L1 and CTLA-4Ig can protect stem cells from rejection in a humanized mouse model (11). However, this approach left the HLA barrier intact, which may result in hyperacute rejection of the engrafted cells precipitated by preexisting anti-HLA antibodies (12, 13). Moreover, CTLA-4Ig can also impair T regulatory cell (Treg) homeostasis and function, thereby possibly jeopardizing the establishment of operational immune tolerance (14, 15).

In addition to adaptive immune responses, innate immune cells, such as NK cells and macrophages, serve an important role in graft rejection (16). A recent report addressed NK-cell–mediated lysis of B2M-deficient cells by expressing a B2M-HLA-E fusion construct (17). However, this strategy did not cover NK cells lacking NKG2A, the inhibitory receptor for HLA-E, the reactivity of which could still be concerning (18, 19). HLA-G, an NK cell inhibitory ligand expressed at the maternal–fetal interface during pregnancy that acts through multiple inhibitory receptors (9, 20), might thus be a better candidate to fully overcome NK cell responses. Moreover, macrophages, which contribute to rejection of transplanted cells, may be controlled by expression of CD47, a "don't-eat-me" signal that prevents cells from being engulfed by macrophages (21, 22); however, this approach has not yet been explored to protect hPSCs and their differentiated derivatives from macrophage engulfment. Furthermore, a convincing strategy to target both adaptive and innate immunity is yet to be proposed.

Here, we employed the CRISPR/Cas9 system to selectively excise the genes encoding the polymorphic HLA class Ia members, HLA-A/-B/-C, and ablated HLA class II expression by targeting *CIITA* in hPSCs. The resulting HLA-deficient, "immune-opaque" cells were further modified to express the immunomodulatory factors PD-L1, HLA-G, and CD47, which target immune surveillance by T cells, NK cells, and macrophages, respectively. Our strategy addresses both adaptive and innate immune responses and, together with other genetic modifications, may ultimately

Significance

To enable cell therapy on a broader scale, the development of universal donor stem cell products that can be administered to multiple patients in need has been proposed, yet a strategy controlling both adaptive and innate immune rejection has not been reported. In this study, we employed multiplex genome editing to selectively ablate the highly polymorphic HLA class Ia and class II molecules and introduced the immunoregulatory factors PD-L1, HLA-G, and CD47 to control T cell- and NK cell-mediated immune responses and macrophage engulfment in vitro and in vivo. Our strategy demonstrates the power of cell engineering and informs future studies aiming to generate "off-the-shelf" universal cell products that may make cell therapy available to a larger pool of patients.

Author contributions: X.H., J.L.S., D.A.M., T.B.M., and C.A.C. designed research; X.H., M.W., S.D., P.J.F., J.H.-R.K., Y.X., A.A., and T.B.M. performed research; X.H., P.H., L.M.R.F., D.A.M., and T.B.M. contributed new reagents/analytic tools; X.H., M.W., S.D., P.J.F., J.H.-R.K., Y.X., L.M.R.F., J.L.S., T.B.M., and C.A.C. analyzed data; and X.H., T.B.M., and C.A.C. wrote the paper.

Reviewers: M.C., Washington University; and D.H.S., Columbia University Medical Center.

Conflict of interest statement: C.A.C. is a founder and chief scientific officer of Sana Biotechnology. D.A.M. is a scientific founder and a board observer of Semma Therapeutics. Neither a reagent nor any funding from these companies was used in this study. Harvard University has filed patent applications that cover these inventions.

[1]M.W. and S.D. contributed equally to this work.

[2]To whom correspondence may be addressed. Email: jlstrom@fas.harvard.edu, tmeissner@fas.harvard.edu, or ccowan@bidmc.harvard.edu.

This article contains supporting information online at www.pnas.org/lookup/suppl/doi:10.1073/pnas.1902566116/-/DCSupplemental.

Published online April 30, 2019.

result in "off-the-shelf" universal cell products suitable for transplantation into any patient.

Results

Selective Ablation of Polymorphic HLA-A/-B/-C and HLA Class II Expression. Given that the human MHC class I genes *HLA-A*, *HLA-B*, and *HLA-C* are highly homologous, designing specific short guide RNAs (sgRNAs) targeting the coding regions of each gene proved challenging. Thus, we employed a dual guide multiplex strategy targeting noncoding regions to excise all three genes from the genome of an hPSC line (HUES8). In the *HLA* locus, *HLA-B* and *HLA-C* are adjacent, whereas *HLA-A* is located nearer the telomere. To simultaneously delete *HLA-B* and *HLA-C*, two sgRNAs were designed upstream of *HLA-B* and downstream of *HLA-C* (Fig. 1*A*). Similarly, to remove *HLA-A*, one sgRNA was designed upstream and another sgRNA downstream of *HLA-A* (Fig. 1*B*). Both deletions were confirmed by PCR amplicons spanning the Cas9 cutting sites (*SI Appendix*, Fig. S1 *A* and *B*). Ablation of HLA-A/-B/-C proteins in the final HLA knockout (KO) clone was verified by flow cytometry (Fig. 1*C*).

To prevent HLA class II expression, we targeted the *CIITA* gene, using a previously reported sgRNA (23). A pair of PCR primers flanking the cleavage site in the first exon of *CIITA* was used to amplify the region spanning the cutting site (Fig. 1*D*). PCR amplicons were Sanger-sequenced to identify biallelic frame shifts (*SI Appendix*, Fig. S1 *C* and *D*). To demonstrate loss of HLA class II expression, we differentiated both WT and KO hPSCs into endothelial cells (ECs). Of note, differentiated WT and KO ECs expressed equivalent levels of the EC marker CD144 (VE-Cadherin), indicating that the differentiation efficiency of the resulting cells was unaffected by genome editing (*SI Appendix*, Fig. S1*E*). Importantly, induction of HLA-DR expression upon IFNγ stimulation was abolished in KO ECs (Fig. 1*E*).

Targeted Integration of Immunomodulatory Factors into the *AAVS1* Safe Harbor Locus. We hypothesized that ablating the polymorphic HLA class Ia and class II molecules would eliminate T cell-mediated adaptive immune rejection. However, HLA-deficient cells would likely still be susceptible to innate immune cells involved in an alloresponse, such as NK cells and macrophages, prompting us to introduce immunomodulatory factors for the following reasons: (*i*) while we left the nonpolymorphic *HLA-E* gene intact, HLA-E surface expression will likely be severely impaired by the removal of polymorphic HLA class Ia genes (24). Thus, failure to express any HLA class I may render donor cells vulnerable to NK-cell–mediated lysis. To protect our engineered cells from NK cells, we sought to introduce HLA-G into the HLA knockout cells. (*ii*) To control macrophage engulfment, we aimed to overexpress CD47. (*iii*) HLA-G can present classical peptides derived from intracellular proteins to T cells (25), which could potentially re-expose our modified cells to $CD8^+$ T cell immune surveillance. Furthermore, γδT cells can directly recognize antigens and initiate a cytotoxic response even in an HLA-null background (26). To counteract any residual T cell activity, we decided to knock in PD-L1, directly suppressing T cell responses (27). Moreover, PD-L1 expression may also contribute to protecting transplanted cells from innate immune rejection by inhibiting $PD\text{-}1^+$ NK cells (28, 29) and $PD\text{-}1^+$ macrophages (30).

To avoid random integration and positional effects on transgene expression, we sought to knock the immunomodulatory factors into the *AAVS1* safe harbor locus (31). We designed two donor plasmids, one containing a PD-L1; HLA-G; CD47 expression cassette and another one containing a PD-L1; CD47 expression cassette, both driven by a CAGGS promoter (Fig. 1*G*). The donor plasmids were electroporated together with a sgRNA targeting the *AAVS1* locus into the $HLA\text{-}A^{-/-}HLA\text{-}B^{-/-}HLA\text{-}C^{-/-}CIITA^{indel/indel}$ KO clone. Integration into the *AAVS1* locus was verified by PCR (*SI Appendix*, Fig. S1*F*). Two clones were isolated following the workflow in *SI Appendix*, Fig. S1*G* and analyzed by flow cytometry; one named KI-PHC that expressed PD-L1, HLA-G, but did not significantly overexpress

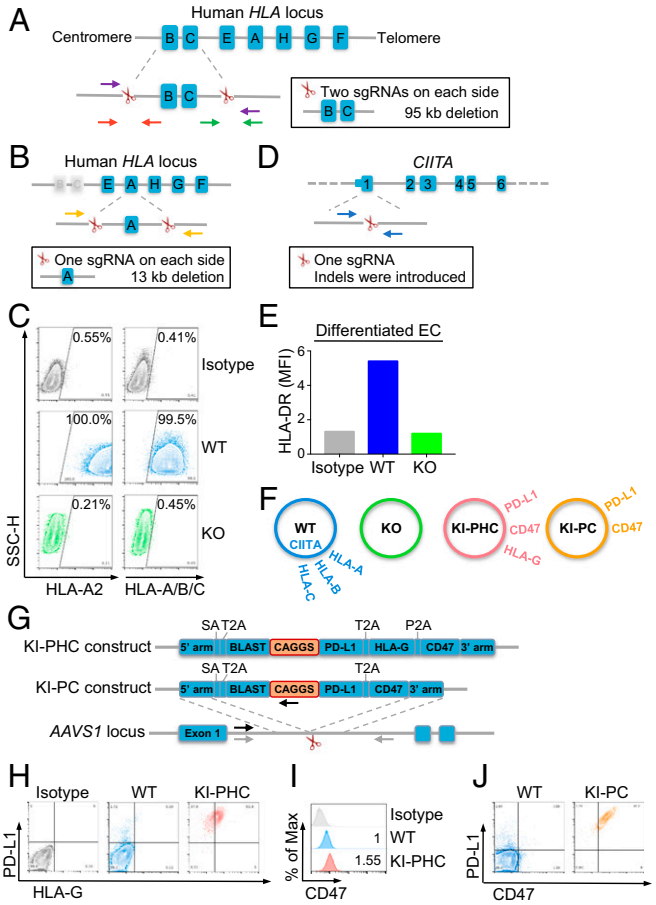

Fig. 1. Genome editing ablates polymorphic HLA-A/-B/-C and HLA class II expression and enables expression of immunomodulatory factors from *AAVS1* safe harbor locus. (*A*) Schematic representation of HLA-B and HLA-C CRISPR/Cas9 knockout strategy. Each pair of scissors represents two sgRNAs. Purple, red, and green arrows indicate primers used for PCR screening. (*B*) Schematic representation of HLA-A knockout strategy. Yellow arrows show primers used for PCR screening. (*C*) FACS plots demonstrating successful ablation of HLA-A/B/C in HUES8. WT or KO hPSCs were treated with IFNγ for 48 h before staining with the indicated antibodies. (*D*) Targeting strategy of *CIITA* locus. Blue arrows indicate primers used for PCR and Sanger sequencing. (*E*) HLA-DR mean fluorescence intensity (MFI) in differentiated $CD144^+$ WT and KO ECs. (*F*) Schematic describing the genotypes of WT, KO, KI-PHC, and KI-PC cell lines. (*G*) Knock-in strategy of immunomodulatory molecules. Scissors represent the sgRNA targeting the *AAVS1* locus. Black and gray arrows indicate primers used for PCR screening. (*H*) PD-L1 and HLA-G expression in KI-PHC hPSCs. (*I*) CD47 expression in KI-PHC cells. MFIs relative to WT cells are indicated on the right of the histograms. (*J*) PD-L1 and CD47 expression in KI-PC hPSCs.

CD47, compared with WT cells (Fig. 1 *H* and *I*), and a second one named KI-PC that expressed PD-L1 and displayed an elevated CD47 level (Fig. 1*J* and *SI Appendix*, Fig. S2*A*). Loss of HLA class Ia and class II expression were confirmed in both KI hPSCs or ECs (*SI Appendix*, Fig. S2 *B–D*). Thus, we successfully inserted immunomodulatory factors into the *AAVS1* safe harbor locus of HLA null cells. Altogether, we generated three engineered hPSC lines: KO, KI-PHC, and KI-PC (Fig. 1*F*).

Next, we sought to confirm the transgene expression in derivatives of the engineered hPSC lines. For this purpose, we differentiated the engineered hPSCs into vascular smooth muscle cells (VSMCs). WT, KO, KI-PHC, and KI-PC VSMCs expressed equivalent levels of the VSMC marker CD140b (PDGFRB), confirming similar differentiation efficiencies (*SI Appendix*, Fig. S2*E*). In KI-PHC VSMCs, we observed a subpopulation with modestly higher expression of PD-L1 and HLA-G, compared with

WT VSMCs, and a major population displaying significantly elevated levels of PD-L1 and HLA-G (*SI Appendix*, Fig. S2*F*). However, we did not observe increased CD47 expression in KI-PHC VSMCs (*SI Appendix*, Fig. S2*F*), which could be a result of incomplete expression from our targeting cassette, where all three gene products are linked by a 2A-peptide (Fig. 1*G*). Similar expression patterns of the transgenes were observed in KI-PC VSMCs (*SI Appendix*, Fig. S2*F*).

To assess whether HLA-E surface trafficking was impaired in the HLA KO background, we stimulated VSMCs with IFNγ and stained the cells with an HLA-E–specific antibody. While WT VSMC drastically up-regulated HLA-E expression, its cell-surface levels were greatly reduced in KO VSMCs (*SI Appendix*, Fig. S2*G*), which was not due to impaired HLA-E gene expression (*SI Appendix*, Fig. S2*H*). Surprisingly, HLA-E surface levels were not restored by HLA-G expression in the KI-PHC VSMCs (*SI Appendix*, Fig. S2*G*), which is inconsistent with a previous report that the HLA-G leader peptide is sufficient to promote HLA-E surface trafficking (32). Nevertheless, HLA-G surface trafficking was unimpaired in KI-PHC VSMCs (*SI Appendix*, Fig. S2*F*), providing further incentive to introduce this tolerogenic factor into our engineered cell products to compensate for the reduction of HLA-E surface expression in an HLA-A/-B/-C null background.

Modified Human Pluripotent Stem Cell Lines Retain Pluripotency and Differentiation Potential. To confirm that our engineered hPSC lines retained pluripotency, expression of NANOG, OCT4, SSEA3, SSEA4, and TRA-1–60 was assessed by immunofluorescence in KO, KI-PHC, and KI-PC hPSCs and was found to be equivalent to that of unmodified hPSCs (Fig. 2*A*). In addition, KO, KI-PHC, and KI-PC hPSCs were differentiated into the three germ layers. qRT-PCR was carried out to examine the expression of ectoderm, mesoderm, and endoderm markers and compared with the three germ layers derived from unmodified hPSCs. All of the lineage markers analyzed were found expressed at similar levels in derivatives of WT as well as of the three engineered cell lines (Fig. 2*B*). In addition, the KO, KI-PHC, and KI-PC hPSCs displayed a normal karyotype (Fig. 2*C*).

To analyze potential off-target effects of the sgRNAs used to engineer our hPSC lines, we PCR-amplified 21 top-ranked in silico predicted exonic off-target sites from the engineered hPSC lines as well as from the parental WT hPSCs. Sanger sequencing of the PCR products did not reveal any unintended edits on these sites except for the pseudogene *HLA-H* (*HFE*), which displayed a perfect match to the sgRNA upstream of *HLA-A* (*SI Appendix*, Figs. S3 and S4). More extensively, we performed target capture sequencing for all of the 648 predicted off-target sites for the eight sgRNAs used in this study. As a result, in addition to 12 naturally occurring SNP/polymorphic sites identified, we confirmed *HLA-H* (*HFE*) as an off-target site in all three cell lines. Moreover, we detected an intronic off-target site in *TRAF3* in all three cell lines resulting from targeting *HLA-C*, as well as an intronic off-target site in *CPNE5* in the KI-PC cell line as a result of the *AAVS1* sgRNA (*SI Appendix*, Figs. S5 and S6 and Dataset S1). Altogether, although three off-target events were detected, our engineered hPSC lines retained pluripotency and their capacity to differentiate into cells of all three germ layers, as well as into VSMCs and ECs with differentiation efficiencies similar to their WT counterparts.

Reduced T Cell Responses Against KO and KI Cell Lines. To investigate whether removing the polymorphic HLA molecules is sufficient to prevent T cell-mediated immune responses, or may be further suppressed by PD-L1, we cocultured WT, KO, or KI-PHC cells with allogeneic T cells from healthy donors. Three in vitro T cell immunoassays were performed: T cell proliferation, activation, and killing assays. Since HLA class I expression is modest in hPSCs (33, 34), we differentiated our engineered as well as WT hPSCs into ECs, which express both HLA class I and II following IFNγ stimulation, or into VSMCs, which express only HLA class I, before using them in the respective immunoassays.

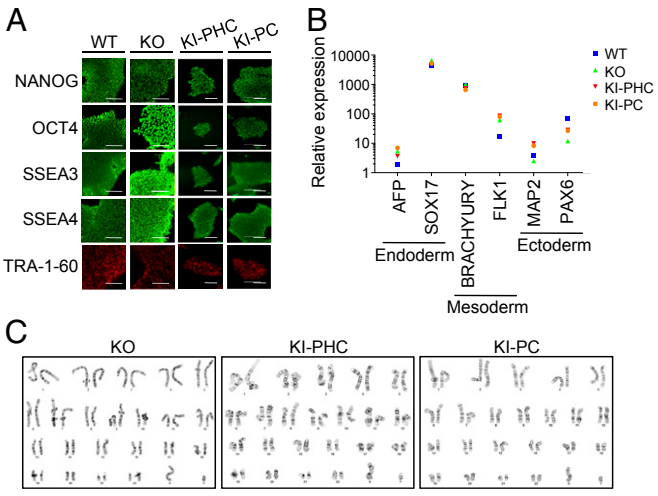

Fig. 2. KO and KI cell lines retain pluripotency and differentiation potential. (*A*) Immunofluorescence indicating that pluripotency markers were expressed by WT, KO, KI-PHC, and KI-PC hPSCs. (Scale bars, 200 μm.) (*B*) qRT-PCR was carried out to survey trilineage markers after WT, KO, KI-PHC, and KI-PC hPSCs were differentiated into the indicated three germ layers. Relative quantification was normalized to each gene level in undifferentiated hPSCs. (*C*) G-banding of chromosomes in KO, KI-PHC, and KI-PC cell lines demonstrated normal karyotypes after successive rounds of genome engineering.

For T cell proliferation assays, WT, KO, and KI-PHC ECs were pretreated with IFNγ and subsequently cocultured with carboxyfluorescein succinimidyl ester (CFSE)-labeled allogeneic $CD3^+$ T cells for 5 d. T cells were then analyzed for dilution of the CFSE signal by flow cytometry as a readout for T cell proliferation in the $CD3/4/8^+$ T cell subpopulations (*SI Appendix*, Fig. S7*A*). FACS plots of one representative T cell donor are shown in *SI Appendix*, Fig. S7*B*. As predicted, the percentage of total proliferating T cells ($CD3^+$) was reduced when incubated with KO ECs (4.17%) or KI-PHC ECs (3.87%) compared with WT ECs (8.29%) (Fig. 3*A*, *Left*). $CD4^+$ T cells followed a similar pattern (Fig. 3*A*, *Middle*). Moreover, $CD8^+$ cytotoxic T cells exhibited significantly reduced proliferation when cocultured with KO ECs (7.71%) or KI-PHC ECs (5.95%), compared with WT ECs (14.32%) (Fig. 3*A*, *Right*). Importantly, compared with cocultures with KO ECs, $CD8^+$ T cells proliferated significantly less in the presence of KI-PHC ECs (Fig. 3*A*, *Right*), indicating that $CD8^+$ T cell activation was suppressed even further by overexpression of PD-L1 in an HLA null background. To further investigate the suppressive role of PD-L1 during the responses of different T cell subpopulations, we transduced hPSCs with an inducible PD-L1 construct and differentiated them into ECs before conducting a T cell proliferation assay. We found that only $CD8^+$, not $CD4^+$, T cell proliferation was reduced in the presence of PD-L1–expressing ECs, compared with WT ECs, arguing for a specific inhibitory effect of PD-L1 on the $CD8^+$ T cell subset (*SI Appendix*, Fig. S7 *C* and *D*).

Utilizing the same coculture of T cells with ECs as target cells, we examined the expression of the early T cell activation marker CD69 in a 3-d coculture and of CD154 (CD40L) in a 5-d coculture (Fig. 3*B*). We found reduced percentages of $CD69^+$ and $CD154^+$ T cells ($CD3^+$) in cocultures with KI-PHC ECs (2.27 and 0.4143%, respectively) or KO ECs (2.303 and 0.65%, respectively), compared with T cells coincubated with WT ECs (7.7 and 7.123%, respectively) (Fig. 3*B*). The same trends were observed in the $CD4^+$ and the $CD8^+$ T cell populations (Fig. 3*B*). However, we did not observe a significantly reduced expression of activation markers in T cells against KI-PHC ECs compared with KO ECs.

To quantify T cell killing, we measured lactate dehydrogenase (LDH) released from VSMCs as a surrogate for T cell cytotoxicity. In this setting, only the $CD8^+$ T cells were expected to be activated

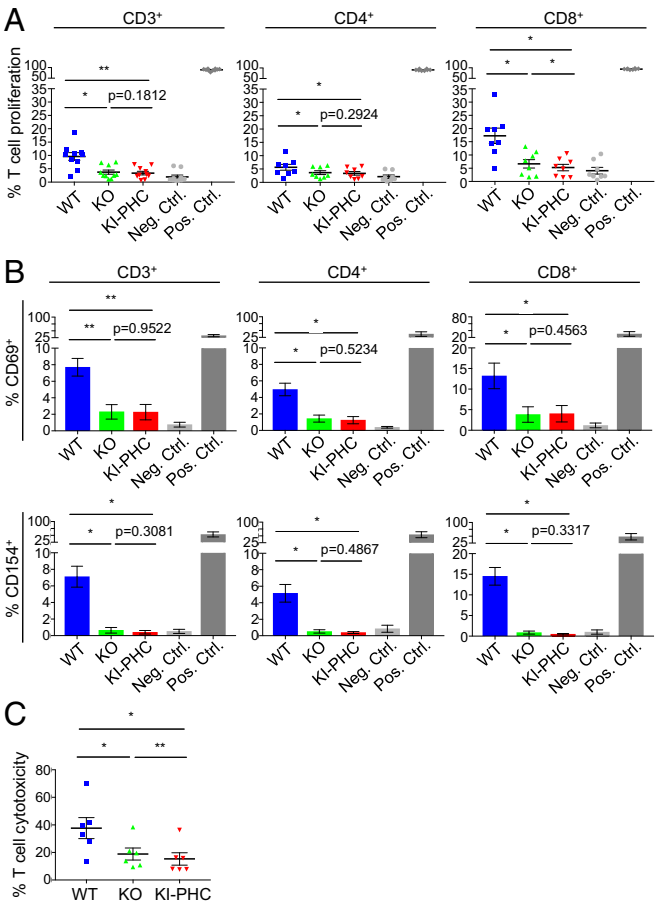

Fig. 3. Reduced T cell activities against KO and KI-PHC cell lines in vitro. (*A*) Scatterplots displaying percentage of proliferating T cells in $CD3^+$ (*Left*, $n = 8$ donors), $CD4^+$ (*Middle*, $n = 6$ donors), and $CD8^+$ T cell (*Right*, $n = 6$ donors) populations when cocultured with WT, KO, or KI ECs. T cells cultured alone were used as negative controls; T cells activated with CD3/CD28 beads served as positive controls. Paired one-way ANOVA followed by Tukey's multiple comparison test. Data are mean ± SEM; $*P < 0.05$; $**P < 0.01$. (*B*) Scatterplot displaying the percentage of $CD69^+$ (*Upper*, $n = 3$ donors) and $CD154^+$ cells (*Lower*, $n = 4$ donors) in $CD3^+$ (*Left*), $CD4^+$ (*Middle*), and $CD8^+$ T cell (*Right*) populations after a coculture with WT, KO, or KI ECs. The same negative and positive controls were used as in *A*. Paired one-way ANOVA followed by Tukey's multiple comparison test. Data are mean ± SEM; $*P < 0.05$; $**P < 0.01$. (*C*) Bar graph representing percentage of T cell cytotoxicity against WT, KO, and KI ECs ($n = 6$ donors). Paired one-way ANOVA followed by Tukey's multiple comparison test. Data are mean ± SEM; $*P < 0.05$; $**P < 0.01$.

by HLA class I-TCR (T cell receptor) engagement, given that VSMCs express solely HLA class I. We found that the $CD8^+$ T cell cytotoxicity against KI-PHC VSMCs (15.31%) was the lowest compared with KO (18.86%) and WT (37.65%) VSMCs (Fig. 3*C*). This observation suggests that the $CD8^+$ T cell cytotoxicity was suppressed even further by PD-L1 expression in KI-PHC VSMCs, consistent with the results of the $CD8^+$ T cell proliferation assay.

To assess T cell responses in vivo, WT and the engineered hPSCs were transplanted s.c. into immunodeficient mice and allowed to form teratomas over the course of 4–6 wk. Presensitized allogeneic $CD8^+$ T cells were then adoptively transferred via tail vein injection and teratoma growth was monitored for an additional 8 d (Fig. 4*A*). As measured by CD69 and PD-1 expression of $CD8^+$ T cells pre- and post priming, the T cells used for injection were activated ($CD69^+$) without signs of exhaustion ($PD\text{-}1^+$) following sensitization (*SI Appendix*, Fig. S8*A*). In agreement with the hypothesis that only the WT cells will be rejected, WT teratomas displayed a slower increase in volume compared with KO teratomas 7 d after injection of $CD8^+$ T cells, which was not due to a slower growth rate of the WT teratoma themselves (Fig. 4 *B* and *C*). These results suggest that the KO teratomas were protected against T cell-mediated rejection. Moreover, although not significant, the average volumes of the KI-PHC and KI-PC teratomas were also larger than that of the WT teratomas 7 d post T cell infusion (Fig. 4*B*). In addition, teratomas derived from both the KO and KI cell lines displayed reduced T cell infiltration, as evidenced by qPCR for the human effector T cell markers CD8 and IL-2 (Fig. 4*D*), as well as by histology (Fig. 4*E*). Together, these observations suggest that removal of the polymorphic HLA molecules from the cell surface of transplanted cells can effectively block T cell-mediated rejection in vivo, matching our in vitro observations.

KI Cell Lines Evade NK Cell and Macrophage Responses. Due to the lack of HLA class Ia molecules and impaired HLA-E surface expression, we expected the HLA KO hPSCs and their derivatives to be vulnerable to NK-cell–mediated lysis, but not the KI-PHC cell line as a result of HLA-G expression. To test our hypothesis, we coincubated allogeneic NK cells from healthy donors with WT, KO, or KI-PHC VSMCs. $CD56^+$ NK cells were analyzed by flow cytometry for surface expression of the degranulation marker CD107a as a readout of NK cell activation (*SI Appendix*, Fig. S8*B*). Of note, NK cell degranulation in the presence of KO VSMCs (13.51%) was not significantly higher than in cocultures with WT VSMCs (10.16%) (Fig. 5*A*), suggesting the lack of an NK cell activation signal on hPSC-derived VSMCs. In agreement with our hypothesis, we found that the percentage of $CD107a^+$ NK cells in cocultures with KI-PHC VSMCs (5.43%) was significantly lower than in KO VSMC cocultures (13.51%) (Fig. 5*A*), suggesting that NK cell activity is indeed inhibited by HLA-G expression in KI-PHC VSMCs. FACS plots of one representative donor are shown in *SI Appendix*, Fig. S8*C*. We also examined LDH released from apoptotic VSMCs after coincubation with NK cells to quantify NK cell cytotoxicity. Consistent with NK cell degranulation, we observed that NK cell cytotoxicity was reduced when NK cells were incubated with KI-PHC VMSCs (Fig. 5*B*).

Finally, we examined macrophage activity using a pH-sensitive fluorescent dye (pHrodo-Red) that emits a signal upon phagocytic engulfment. We hypothesized that overexpression of CD47 in KI-PC VSMCs would reduce macrophage engulfment. As a positive control, a CD47 knockout ($CD47^{-/-}$) cell line was generated, and loss of CD47 cell-surface expression was verified by flow cytometry (*SI Appendix*, Fig. S8*D*). pHrodo-Red–labeled VSMCs differentiated from WT, $CD47^{-/-}$, and KI-PC cells were either treated with staurosporine (STS) to induce apoptosis or left untreated and then incubated with monocyte-derived macrophages from healthy donors. The emergence of red signal, an indicator of VSMC engulfment by macrophages, was monitored by live cell imaging, and the fluorescence intensity was quantified. Of note, with or without STS treatment, KI-PC VSMCs displayed significantly decreased engulfment by macrophages compared with $CD47^{-/-}$ or WT VSMCs (Fig. 5 *C* and *D* and *SI Appendix*, Fig. S8*E*). These data demonstrate that overexpression of CD47 can indeed minimize macrophage engulfment of engineered hPSC-derived VSMCs.

Discussion

In this study, we applied multiplex CRISPR/Cas9 genome editing to render hPSC hypoimmunogenic to both adaptive and innate immune responses. We specifically deleted the highly polymorphic HLA-A/-B/-C genes and prevented the expression of HLA class II genes by targeting *CIITA*. In addition, we introduced the immunomodulatory factors PD-L1, HLA-G, and CD47 into the *AAVS1* safe harbor locus. We found that engineered hPSC derivatives elicited significantly less immune activation and killing by T cells and NK cells and displayed minimal engulfment by macrophages.

During the gene modification process, a 95-kb deletion was generated that, in addition to the HLA-B/-C genes, also harbors MIR6891 and four pseudogenes. Moreover, one exonic off-target

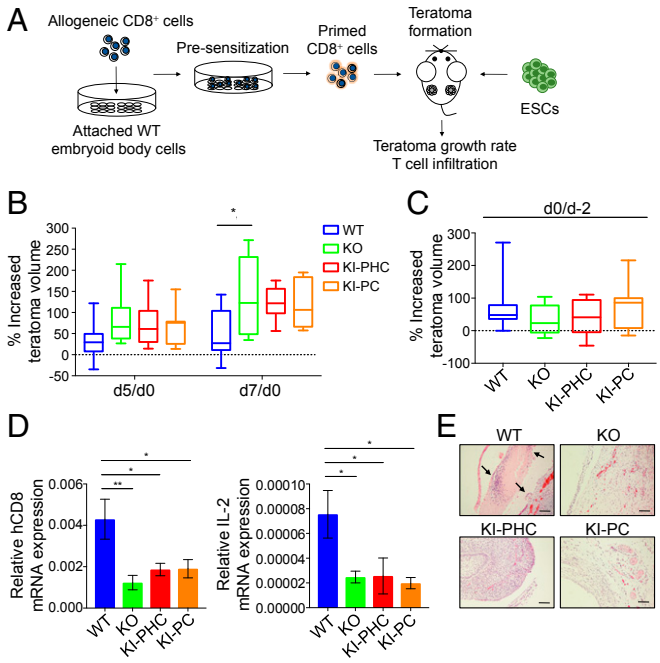

Fig. 4. Reduced T cell responses against KO and KI cell lines in vivo. (*A*) Schematic describing the presensitization of allogeneic CD8$^+$ T cells and in vivo T cell recall response assay. (*B*) Percentage of increased teratoma volume on day 5 or 7 post T cell injection compared with day 0. Genotype of teratoma: WT ($n = 9$), KO ($n = 7$), KI-PHC ($n = 6$), and KI-PC ($n = 7$). Ordinary one-way ANOVA followed by Tukey's multiple comparison test. Data are mean ± SEM; $*P < 0.05$. (*C*) Percentage of increased teratoma volume on day 0 of T cell injection compared with 2 d preinjection. Genotype of teratoma: WT ($n = 9$), KO ($n = 7$), KI-PHC ($n = 6$), and KI-PC ($n = 7$). (*D*) Relative hCD8 (*Left*) and IL-2 (*Right*) mRNA expression in WT ($n = 8$), KO ($n = 7$), KI-PHC ($n = 6$), and KI-PC ($n = 7$) teratomas harvested on day 8 post T cell injection. The expression was normalized to RPLP0. Ordinary one-way ANOVA followed by Tukey's multiple comparison test. Data are mean ± SEM; $*P < 0.05$; $**P < 0.01$. (*E*) Representative hematoxylin and eosin staining of WT, KO, KI-PHC, and KI-PC teratomas harvested on day 8 post T cell injection. Black arrows indicate the sites of T cell infiltration. (Scale bars, 100 μm.)

event was observed in the transcribed pseudogene *HLA-H*, yet these genomic alterations did not impact the growth rate or differentiation efficiencies of the KO and KI cell lines.

As expected, the removal of polymorphic HLA expression in hPSCs and their derivatives, ECs and VSMCs, resulted in reduced T cell responses in vitro and in vivo (Figs. 3 and 4). An interesting observation from our T cell assays is that overexpression of the checkpoint inhibitor PD-L1 had a significant impact only on the proliferation and cytotoxicity of CD8$^+$ T cells (Fig. 3*A*). This may have several possible explanations: (*i*) the levels of the PD-L1 receptor, PD-1, are higher on CD8$^+$ T cells than on CD4$^+$ T cells and (*ii*) CD8$^+$ T cells are the cell type most responsive to target cell exposure in our assays and hence will also express higher levels of the negative regulator PD-1. Moreover, we noted that this inhibitory effect of PD-L1 on CD8$^+$ T cell proliferation occurred even in the absence of HLA (Fig. 3*A*), suggesting that HLA-TCR interaction is not required for PD-L1 to act as a tolerogenic factor. Interestingly, in all three in vitro T cell immunoassays, we still observed residual T cell activity even in cocultures with the KI-PHC cell line, compared with the negative control (Fig. 3), and thus T cell responses to these cells appeared blunted but not eliminated. This is most likely due to the experimental setup, considering that target cells may secrete factors that promote T cell activation independently of the presence of HLA. Alternatively, the residual T cell activity may be a result of the modifications in our cell lines, which may have introduced additional antigens recognizable by the immune system.

While acute graft rejection is mainly T cell-mediated, the role of other immune cells such as macrophages, NK cells, and B cells must also be considered with regards to long-term survival of therapeutic cells. Our NK cell assays suggest that HLA-G expression was able to control NK cell activities, although the contribution of PD-L1 in our experimental setup cannot be ruled out without the use of an HLA-G–blocking antibody in this assay. Similarly, overexpression of CD47 in combination with PD-L1 effectively reduced macrophage engulfment. With regards to long-term engraftment, in particular, antibody-dependent cellular cytotoxicity by NK cells and allo-antibody–mediated complement activation as the main drivers of chronic graft rejection must be considered in the future (35–37). While various humanized mouse models exist to assess the immunogenicity of transplanted cells, they are limited in recapitulating a full immune response. Therefore, the development of improved in vivo models for testing cell transplantation and rejection is imperative (38–41).

Finally, overcoming the immune barrier to transplantation would also provide an exciting new modality to treat autoimmune

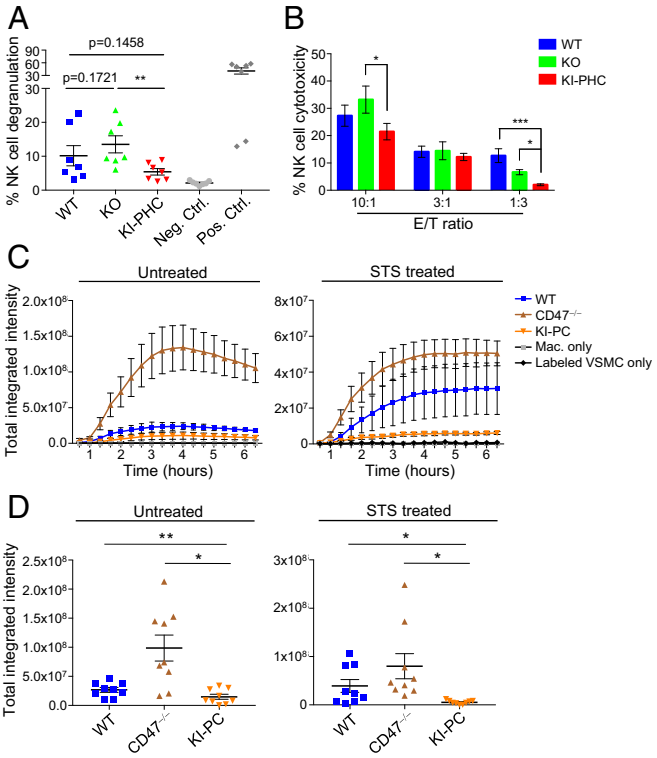

Fig. 5. KI cell lines are protected from NK cell and macrophage responses. (*A*) Scatterplot of percentage of CD56$^+$CD107a$^+$ cells as a readout for NK cell degranulation against WT, KO, or KI-PHC VSMCs ($n = 7$ donors). NK cells cultured alone were used as negative control; NK cells treated with PMA/ionomycin served as positive control. Paired one-way ANOVA followed by Tukey's multiple comparison test. Data are mean ± SEM; $**P < 0.01$. (*B*) Bar graph representing the percentage of NK cytotoxicity against WT, KO, and KI-PHC VSMCs from one representative donor at the indicated effector/target (E/T) ratios ($n = 3$ replicates). Unpaired one-way ANOVA followed by Tukey's multiple comparison test. Data are mean ± SD; $*P < 0.05$; $***P < 0.001$. (*C*) Time-lapse plots of macrophage phagocytosis assay ($n = 5$ monocyte donors). pHrodo-red–labeled VSMCs of indicated genotypes that were pretreated (*Right*) or not pretreated (*Left*) with STS were coincubated with monocyte-derived macrophages for 6 h. Images were acquired every 20 min using a live cell imaging system. Total integrated fluorescence intensity of pHrodo-red$^+$ phagosomes per image was analyzed. Data are mean ± SEM. (*D*) Scatterplots of macrophage phagocytosis assay at 4 h coincubation ($n = 9$ monocyte donors, three independent experiments). The experimental conditions were the same as in *C*. Paired one-way ANOVA followed by Tukey's multiple comparison test. Data are mean ± SEM; $*P < 0.05$; $**P < 0.01$.

diseases such as type 1 diabetes and multiple sclerosis, where one particular cell type is attacked by the patient's immune system and needs replacement. Thus, the generation of cells that can be safely transplanted into anyone, without immune rejection, holds the promise of unlocking the full potential of regenerative medicine.

Materials and Methods

Detailed materials and methods are described in *SI Appendix, Supplementary Materials and Methods*.

The use of human pluripotent stem cells was approved by the Embryonic Stem Cell Research Oversight Committee (ESCRO), Harvard University. All human blood samples used for this study were deidentified, discarded clinical material. The Committee on the Use of Human Subjects [the Harvard institutional review board (IRB)] determined that this use is exempt from the requirements of IRB review. All animal experiments were performed in accordance to Harvard University International Animal Care and Use Committee regulations.

Human ES Cell Culture and EC and VSMC Differentiation. HUES8 cells (42) were grown on Geltrex (Life Technologies)-coated plates in mTeSR1 (StemCell Technologies). Cells were passaged with Gentle Cell Dissociation Reagent (StemCell Technologies) and replated in media supplemented with RevitaCell (ThermoFisher Scientific). Human ECs and VSMCs were differentiated following our previously published protocols (43).

T Cell Assays. To assess T cell proliferation, $CD3^+$ T cells were labeled with CellTrace CFSE (ThermoFisher Scientific). ECs were pretreated with IFNγ before coincubation with CFSE-labeled T cells for 5 d in media supplemented with 20 U/mL IL-2. T cells were then stained with anti-CD3/4/8 antibodies before CFSE intensity was analyzed on a LSR II. The T cell activation markers CD69 and CD154 were analyzed 3 and 5 d after coculture, respectively. T cell killing was assessed following a 5-d coculture with VSMCs at the indicated effector/target ratio. Supernatants were analyzed by the Pierce LDH Cytotoxicity Assay Kit (ThermoFisher Scientific) following the manufacturer's instructions.

NK Cell Assays. NK cell degranulation was determined as described in ref. 44. NK cells were stained with α-CD56 PE (Biolegend), and CD107a surface expression was analyzed on a FACSCalibur. NK killing activity was determined using the Pierce LDH Cytotoxicity Assay Kit (ThermoFisher Scientific) following the manufacturer's instructions.

Macrophage Phagocytosis Assay. VSMCs were pretreated with 200 nM staurosporine (Sigma) or left untreated and subsequently dissociated and labeled with pHrodo-Red (IncuCyte). Labeled VSMCs were added to human monocyte-derived macrophages, and cocultures were imaged using the Celldiscover 7 live cell imaging platform (Zeiss). Total integrated intensity (mean fluorescence intensity × total area) was analyzed using the ZEN imaging software (Zeiss).

Statistical Analyses. Statistical analyses were performed using Prism 7 (Graphpad).

ACKNOWLEDGMENTS. We thank Dr. Bin Gui (Brigham and Women's Hospital) for help with next-generation sequencing-based off-target analysis and Caroline Becker (iPSC core, Harvard Stem Cell Institute) for advice on pluripotency assays. This work was supported by awards from the Harvard Stem Cell Institute and the Blavatnik Biomedical Accelerator Program, as well as the Juvenile Diabetes Research Foundation.

1. de Rham C, Villard J (2014) Potential and limitation of HLA-based banking of human pluripotent stem cells for cell therapy. *J Immunol Res* 2014:518135.
2. Tapia N, Schöler HR (2016) Molecular obstacles to clinical translation of iPSCs. *Cell Stem Cell* 19:298–309.
3. Mandal PK, et al. (2014) Efficient ablation of genes in human hematopoietic stem and effector cells using CRISPR/Cas9. *Cell Stem Cell* 15:643–652.
4. Meissner TB, Mandal PK, Ferreira LM, Rossi DJ, Cowan CA (2014) Genome editing for human gene therapy. *Methods Enzymol* 546:273–295.
5. Riolobos L, et al. (2013) HLA engineering of human pluripotent stem cells. *Mol Ther* 21:1232–1241.
6. Wang D, Quan Y, Yan Q, Morales JE, Wetsel RA (2015) Targeted disruption of the β2-microglobulin gene minimizes the immunogenicity of human embryonic stem cells. *Stem Cells Transl Med* 4:1234–1245.
7. Mattapally S, et al. (2018) Human leukocyte antigen class I and II knockout human induced pluripotent stem cell-derived cells: Universal donor for cell therapy. *J Am Heart Assoc* 7:e010239.
8. Chen H, et al. (2015) Functional disruption of human leukocyte antigen II in human embryonic stem cell. *Biol Res* 48:59.
9. Ferreira LMR, Meissner TB, Tilburgs T, Strominger JL (2017) HLA-G: At the interface of maternal-fetal tolerance. *Trends Immunol* 38:272–286.
10. Lee N, et al. (1998) HLA-E is a major ligand for the natural killer inhibitory receptor CD94/NKG2A. *Proc Natl Acad Sci USA* 95:5199–5204.
11. Rong Z, et al. (2014) An effective approach to prevent immune rejection of human ESC-derived allografts. *Cell Stem Cell* 14:121–130.
12. Masson E, et al. (2007) Hyperacute rejection after lung transplantation caused by undetected low-titer anti-HLA antibodies. *J Heart Lung Transplant* 26:642–645.
13. Iniotaki-Theodoraki A (2001) The role of HLA class I and class II antibodies in renal transplantation. *Nephrol Dial Transplant* 16:150–152.
14. Bour-Jordan H, et al. (2004) Costimulation controls diabetes by altering the balance of pathogenic and regulatory T cells. *J Clin Invest* 114:979–987.
15. Salomon B, Bluestone JA (2001) Complexities of CD28/B7: CTLA-4 costimulatory pathways in autoimmunity and transplantation. *Annu Rev Immunol* 19:225–252.
16. LaRosa DF, Rahman AH, Turka LA (2007) The innate immune system in allograft rejection and tolerance. *J Immunol* 178:7503–7509.
17. Gornalusse GG, et al. (2017) HLA-E-expressing pluripotent stem cells escape allogeneic responses and lysis by NK cells. *Nat Biotechnol* 35:765–772.
18. Braud VM, et al. (1998) HLA-E binds to natural killer cell receptors CD94/NKG2A, B and C. *Nature* 391:795–799.
19. Pegram HJ, Andrews DM, Smyth MJ, Darcy PK, Kershaw MH (2011) Activating and inhibitory receptors of natural killer cells. *Immunol Cell Biol* 89:216–224.
20. Pazmany L, et al. (1996) Protection from natural killer cell-mediated lysis by HLA-G expression on target cells. *Science* 274:792–795.
21. Chhabra A, et al. (2016) Hematopoietic stem cell transplantation in immunocompetent hosts without radiation or chemotherapy. *Sci Transl Med* 8:351ra105.
22. Jaiswal S, et al. (2009) CD47 is upregulated on circulating hematopoietic stem cells and leukemia cells to avoid phagocytosis. *Cell* 138:271–285.
23. Ding Q, et al. (2013) Enhanced efficiency of human pluripotent stem cell genome editing through replacing TALENs with CRISPRs. *Cell Stem Cell* 12:393–394.
24. Braud VM, Allan DS, Wilson D, McMichael AJ (1998) TAP- and tapasin-dependent HLA-E surface expression correlates with the binding of an MHC class I leader peptide. *Curr Biol* 8:1–10.
25. Diehl M, et al. (1996) Nonclassical HLA-G molecules are classical peptide presenters. *Curr Biol* 6:305–314.
26. Vantourout P, Hayday A (2013) Six-of-the-best: Unique contributions of γδ T cells to immunology. *Nat Rev Immunol* 13:88–100.
27. Riley JL (2009) PD-1 signaling in primary T cells. *Immunol Rev* 229:114–125.
28. Beldi-Ferchiou A, et al. (2016) PD-1 mediates functional exhaustion of activated NK cells in patients with Kaposi sarcoma. *Oncotarget* 7:72961–72977.
29. Della Chiesa M, et al. (2016) Features of memory-like and PD-1(+) human NK cell subsets. *Front Immunol* 7:351.
30. Gordon SR, et al. (2017) PD-1 expression by tumour-associated macrophages inhibits phagocytosis and tumour immunity. *Nature* 545:495–499.
31. Sadelain M, Papapetrou EP, Bushman FD (2011) Safe harbours for the integration of new DNA in the human genome. *Nat Rev Cancer* 12:51–58.
32. Lee N, Goodlett DR, Ishitani A, Marquardt H, Geraghty DE (1998) HLA-E surface expression depends on binding of TAP-dependent peptides derived from certain HLA class I signal sequences. *J Immunol* 160:4951–4960.
33. Drukker M, et al. (2002) Characterization of the expression of MHC proteins in human embryonic stem cells. *Proc Natl Acad Sci USA* 99:9864–9869.
34. de Almeida PE, Ransohoff JD, Nahid A, Wu JC (2013) Immunogenicity of pluripotent stem cells and their derivatives. *Circ Res* 112:549–561.
35. Michaels PJ, Fishbein MC, Colvin RB (2003) Humoral rejection of human organ transplants. *Springer Semin Immunopathol* 25:119–140.
36. Djamali A, et al. (2014) Diagnosis and management of antibody-mediated rejection: Current status and novel approaches. *Am J Transplant* 14:255–271.
37. Baldwin WM, III, Valujskikh A, Fairchild RL (2016) Mechanisms of antibody-mediated acute and chronic rejection of kidney allografts. *Curr Opin Organ Transplant* 21:7–14.
38. Melkus MW, et al. (2006) Humanized mice mount specific adaptive and innate immune responses to EBV and TSST-1. *Nat Med* 12:1316–1322.
39. Rongvaux A, et al. (2014) Development and function of human innate immune cells in a humanized mouse model. *Nat Biotechnol* 32:364–372.
40. Brehm MA, Wiles MV, Greiner DL, Shultz LD (2014) Generation of improved humanized mouse models for human infectious diseases. *J Immunol Methods* 410:3–17.
41. Li Y, et al. (2018) A human immune system mouse model with robust lymph node development. *Nat Methods* 15:623–630.
42. Cowan CA, et al. (2004) Derivation of embryonic stem-cell lines from human blastocysts. *N Engl J Med* 350:1353–1356.
43. Patsch C, et al. (2015) Generation of vascular endothelial and smooth muscle cells from human pluripotent stem cells. *Nat Cell Biol* 17:994–1003.
44. Andzelm MM, Chen X, Krzewski K, Orange JS, Strominger JL (2007) Myosin IIA is required for cytolytic granule exocytosis in human NK cells. *J Exp Med* 204:2285–2291.